

Lawrence Berkeley National Laboratory

Lawrence Berkeley National Laboratory

Title

Three-Dimensional Laser Cooling

Permalink

<https://escholarship.org/uc/item/820331sf>

Author

Okamoto, H.

Publication Date

2008-09-19



Lawrence Berkeley Laboratory

UNIVERSITY OF CALIFORNIA

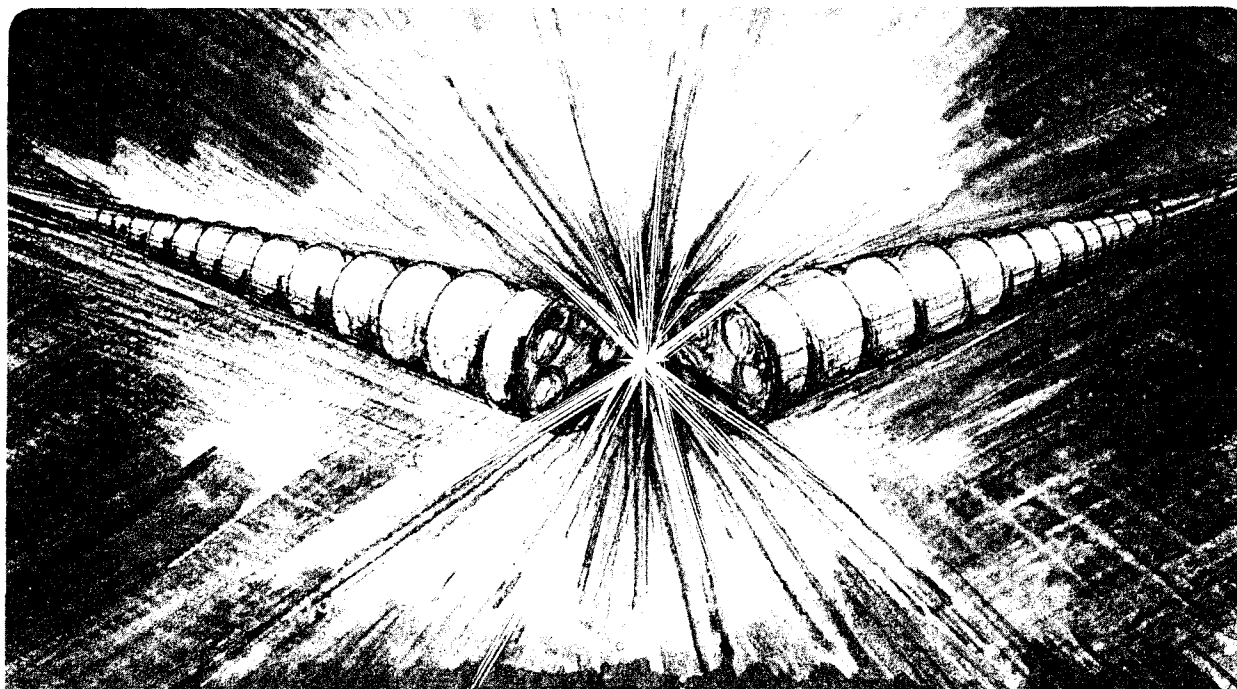
Accelerator & Fusion Research Division

Presented at the European Particle Accelerator Conference,
London, England, June 27–July 1, 1994, and to be published
in the Proceedings

Three-Dimensional Laser Cooling

H. Okamoto, A.M. Sessler, and D. Möhl

June 1994



LOAN COPY
Circulates
for 4 weeks

Bldg. 50 Library
Copy 2

LBL-35899

Three-Dimensional Laser Cooling[†]

Hiromi Okamoto*, Andrew M. Sessler
Lawrence Berkeley Laboratory
1 Cyclotron Road, Berkeley, CA 94720, U.S.A.

Dieter Möhl
CERN-PS, CH 1211
Geneva 23, Switzerland

Abstract

To realize effective *transverse* laser cooling simultaneously with longitudinal laser cooling, two possibilities are theoretically studied. The schemes are both based on forced synchro-betatron coupling, which transfer the extremely effective longitudinal laser cooling action to transverse directions. The coupling is provided by an rf-cavity with a transverse variation of the longitudinal electric field (e.g. TM₂₁₀ mode) or by a normal rf-cavity located at a position of finite dispersion. It is shown that, when a working point is close to the difference resonance, cooling in all three degrees of freedom is simultaneously obtained.

1. INTRODUCTION

Electron cooling and stochastic cooling are well-established techniques, which have been successfully applied to decreasing the temperature of stored beams of anti-protons as well as other particles. A new method, called laser cooling[1], has recently been employed, experimentally, in the TSR Storage Ring of Heidelberg[2] and in the ASTRID Ring of Aarhus[3]. Longitudinal temperature of close to 1 mK, the lowest circulating beam temperature ever reported, have been achieved for ⁷Li⁺. The laser cooling mechanism is, however, applicable only to longitudinal motion, and no effective method to realize simultaneous cooling in both longitudinal and transverse motion has, so far, been developed. Thus in the experiments mentioned the longitudinal temperature was 1 mK, but the transverse temperature was 1000 K.

In the present paper, we explore two possible schemes to achieve three-dimensional laser cooling based on forced synchro-betatron coupling.[4,5]. In principle, with only minor modifications in the hardware of the ring, it should be possible to cool transverse beam temperature to the same order as the longitudinal temperature.

If the present schemes work as theoretically expected, it should be possible to observe beam crystallization[6,7]. In addition, laser-cooled beams with ultra-low temperatures could be employed to cool another beam, just analogous to the electron cooling scheme.

This work was supported in part by the Director, Office of Energy Research, Office of High Energy and Nuclear Physics, of the U.S. Department of Energy under contract no. DE-AC03-76 SF00098.

*On leave from Accelerator Laboratory, Institute for Chemical Research, Kyoto University, Gokanoshou, Uji, Kyoto 611, Japan.

2. A COUPLING CAVITY

2.1 Rf cavities

As a source for developing synchro-betatron coupling, let us first consider a *coupling cavity* excited with TM₂₁₀ mode. Assuming a simple rectangular pill-box geometry, the vector potential is given by

$$\mathbf{A}_c = \left(0, 0, \frac{V_c}{\omega_c} \sin\left(\frac{\pi x}{a}\right) \cos\left(\frac{\pi y}{2b}\right) \sin(\omega_c t) \right), \quad (1)$$

where $2a$ and $2b$ are, respectively, the width and height of the cavity, V_c is the voltage amplitude of the rf field, and ω_c denotes the rf angular frequency (harmonic number h_c). Since the longitudinal electric field derived from Eq.(1) near the center has a linear horizontal (x) dependence, we obtain a coupling between the synchrotron motion and horizontal betatron motion.

In order to achieve enhanced coupling, it is necessary to force stored ions to execute synchrotron oscillations. Thus we need to introduce an rf *bunching cavity* which is an ordinary cavity excited either with a coaxial or TM₀₁₀ mode. We write the vector potential as

$$\mathbf{A}_b = \left(0, 0, \frac{V_b}{\omega_b} \sin(\omega_b t) \right), \quad (2)$$

where ω_b and V_b are, respectively, the angular frequency (harmonic number h_b) and voltage amplitude of the bunching cavity.

2.2 Equations of motion

Taking a linear approximation, and assuming zero-dispersion and zero-derivative of it at the cavity, the Hamiltonian of the system including the coupling and bunching cavities can be given as [8]

$$\begin{aligned} H_1 = & \frac{1}{2}(p_x^2 + v_x^2 x^2) \\ & - \frac{\xi_0 W^2}{2} + \frac{2\pi\bar{v}_L^2}{\xi_0} \sin(\psi + \psi_b) \delta_p(\theta - \theta_b) \\ & - \frac{2\pi h_b \Gamma_c}{h_c} x \cdot \sin\left(\frac{h_c}{h_b} \psi + \psi_c\right) \delta_p(\theta - \theta_c). \end{aligned} \quad (3)$$

Here q is the charge state of stored ions, $\xi_0 = \gamma_{tr}^{-2} \gamma^{-2}$ is the phase slip (or off-momentum) factor which always takes a negative value in our applications, v_x is the horizontal tune, \bar{v}_L is related to the longitudinal tune v_L as $\cos(2\pi v_L) = 1 - 2\pi^2 \bar{v}_L^2$, ψ_b and ψ_c are the synchronous phases at the bunching and coupling cavity respectively. The canonical

variables (x, p_x) correspond to the horizontal displacement and momentum, and (ψ, W) to the phase and energy deviation from the synchronous values. The coupling strength has been introduced as $\Gamma_c \equiv qV_c R / 2\beta_0 c p_0 a$, where R represents the average ring radius, and p_0 is the reference particle momentum. In Eq.(3), the independent variable is taken as $\theta = s/R$ with s being the distance along the reference particle orbit, and θ_b and θ_c indicating the location of the bunching and coupling cavity respectively.

To couple the vertical motion to the other two motions, it is only necessary to install a skew quadrupole or a vertical coupling cavity in the ring, but, in this section, we consider, for simplicity, only longitudinal-horizontal coupling.

The Hamiltonian (3) yields the equations of motion

$$\frac{d^2 x}{d\theta^2} + v_x^2 x = 2\pi\Gamma_c \psi \delta_p(\theta - \theta_c), \quad (4)$$

$$\frac{d^2 \psi}{d\theta^2} + 2\pi\bar{v}_L^2 \psi \delta_p(\theta - \theta_b) = -2\pi\xi_0 \Gamma_c x \delta_p(\theta - \theta_c), \quad (5)$$

where we have assumed that $\psi_b = \pi/2$ and $\psi_c = 0$. In our model, the simple frictional term, $\epsilon\Lambda(d\psi/d\theta)$, is added to the l.h.s. of Eq.(5) to incorporate the laser cooling effect. Here, $\epsilon=1$ in the laser cooling section, while $\epsilon=0$ in other regions. This modeling of laser cooling is only approximate (it does not include the variation of cooling force with longitudinal velocity and it does not differentiate between the cooling of longitudinal velocity and the cooling of energy), but the approximation made is adequate for the analysis of this paper.

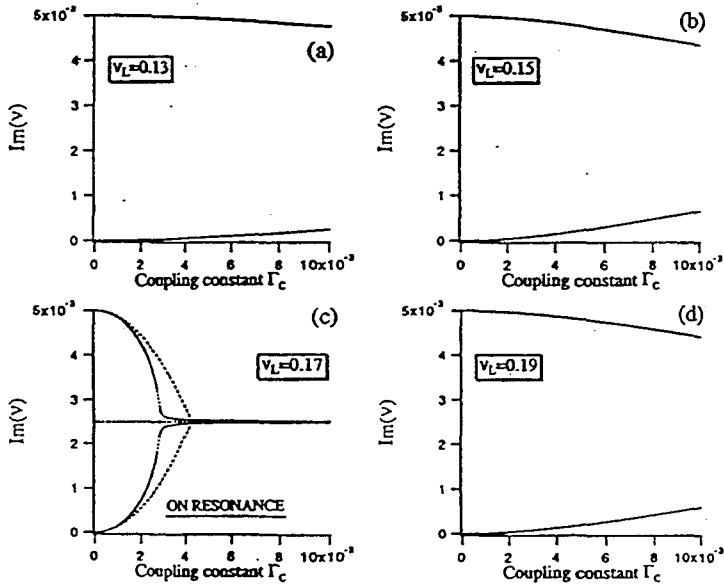


Fig.1 The damping rates, $\text{Im}(v)$, of the longitudinal and transverse modes plotted as a function of the coupling strength Γ_c for three different synchrotron tunes. The horizontal tune and the damping parameter are fixed, respectively, at $v_x = 2.17$ and $\Lambda_D/2\pi = 0.01$. The coupling cavity and bunching cavity are next to each other, and are set at the position opposite to the cooling section. The dotted curves in Fig.1(c) correspond to Eqs.(6). The slip factor is taken to be -0.947 roughly corresponding to the ASTRID ring in Denmark[3].

2.3 Damping rates

Since the motions governed by Eqs.(4) and (5) with the damping term are linear, we can construct the transfer matrix of each element. Figs.1 show the damping rates evaluated from the eigenvalues of the one-turn matrix. It is seen that, only when the operating point is on a difference resonance, i.e. $v_x - v_L = \text{integer}$, the damping of both modes saturate at the level which is exactly half of the maximum longitudinal rate. The condition of resonance must, therefore, be closely satisfied to enhance the horizontal damping.

The dispersion relation from the one-turn transfer matrix can be approximately solved to give the damping rates of the longitudinal and horizontal motion

$$\text{Im}(v) \approx \begin{cases} \frac{\pi^2 |\xi_0| \Gamma_c^2}{v_x} \coth\left(\frac{\Lambda_D}{2}\right), \\ \frac{\Lambda_D}{4\pi} - \frac{\pi^2 |\xi_0| \Gamma_c^2}{v_x} \coth\left(\frac{\Lambda_D}{2}\right), \end{cases} \quad (6)$$

where, we have assumed the resonance condition, taken $\Lambda_D = \Lambda \times$ (the extent of the cooling section), and employed a perturbation analysis assuming $\Gamma_c^2 \ll 1$.

The tracking result corresponding to the case (c) in Fig.1 is shown in Fig.2, using the coupling constant $\Gamma_c = 0.006$. The damping of the both motions is beautifully demonstrated.

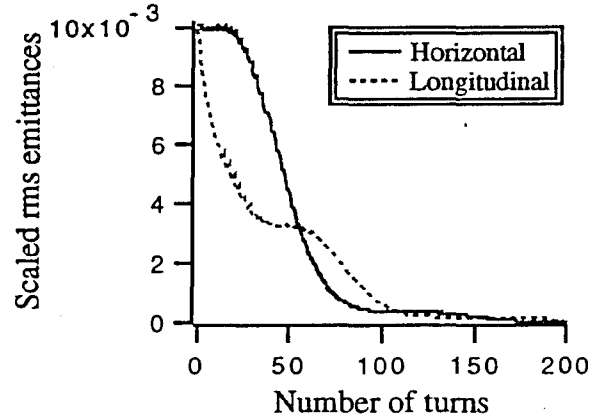


Fig.2 Tracking result corresponding to the parameters employed in Fig.1(c) with $\Gamma_c = 0.006$.

3. DISPERSION-INDUCED COUPLING

3.1 Hamiltonian

Let us now investigate transverse laser cooling induced through dispersion at an rf cavity. We here take vertical motion in to account, introducing a pure skew quadrupole. The Hamiltonian of the system is given by

$$H_2 = \frac{1}{2}(p_x^2 + v_x^2 x^2) + \frac{1}{2}(p_y^2 + v_y^2 y^2) - \frac{\xi_0 W^2}{2} + \Gamma_q xy \cdot \delta_p(\theta - \theta_q) - \frac{h_b q V_b}{p_0 \beta_0 c} \cos(\psi - \zeta_b p_x) \delta_p(\theta - \theta_b), \quad (7)$$

where θ_q is the location of the skew quadrupole magnet having the coupling strength Γ_q . The dispersion function evaluated at the skew quadrupole position θ_q and the

derivative of the dispersion at the cavity position θ_b have been assumed to be zero, and $\zeta_b = \eta(\theta = \theta_b)/R$.

The equation of motion can be readily derived from Eq.(7). The equation for the variable W is, however, modified, incorporating the laser damping effect, as

$$\frac{dW}{d\theta} = \frac{2\pi\bar{v}^2}{\xi_0} \sin(\psi - \zeta_b p_x) \delta_p(\theta - \theta_b) - \epsilon \Lambda W. \quad (8)$$

3.2 Damping rates

Two separate resonance conditions are necessary now; $v_x - v_L = \text{integer}$ for the longitudinal-horizontal coupling, and $v_x - v_y = \text{integer}$ for the horizontal-vertical coupling.

Then, using perturbation analysis with respect to small ζ_b^2 , one obtains the damping rates of the transverse modes

$$\text{Im}(v) = \frac{v_x \bar{v}_L^2 \zeta_b^2}{4|\xi_0|} \tan \frac{\mu_0}{2} \left/ \left(\tanh \frac{\Lambda_D}{2} + \frac{\Gamma_q^2}{2v_x v_y \sinh \Lambda_D} \right) \right., \quad (9)$$

where we have assumed $\Gamma_q / \sqrt{v_x v_y} \ll 1$, putting that $v_x = \mu_0$, $v_y = \mu_0 + 2m\pi$, and $v_L = \mu_0 + 2n\pi$ ($m, n = \text{integer}$). From Figs.3, which give numerical evaluation of all three damping rates, one concludes that there is an *optimum* dispersion for which the three rates become equal.

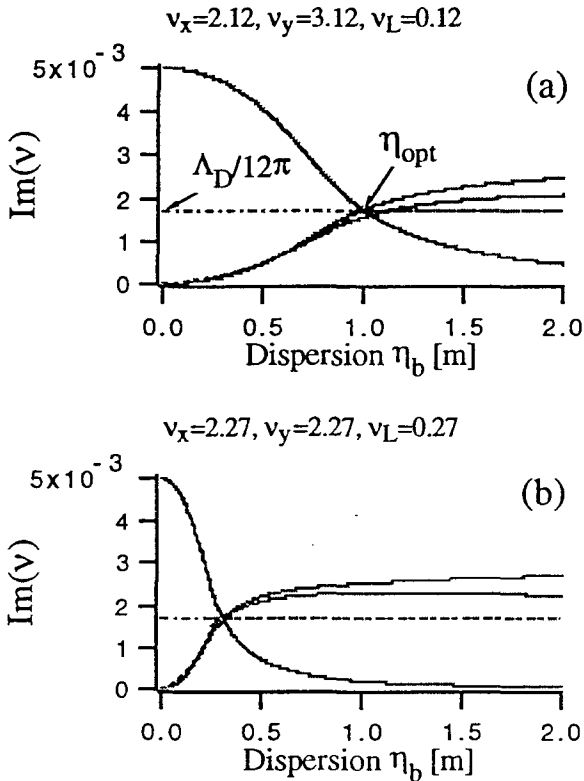


Fig.3 The damping rates, $\text{Im}(v)$, of the longitudinal and transverse modes plotted as a function of the dispersion at the rf-cavity $\eta_b = \eta(\theta = \theta_b)$. The rf-cavity sits at $\theta_b = \pi$, the position opposite to the cooling section, while the quadrupole with the coupling strength $\Gamma_q = 0.1$ is set at $\theta_q = 3\pi/2$. The dotted curves correspond to Eq.(9), and the line parallel to the abscissa indicates the level $\text{Im}(v) = \Lambda_D/12\pi$.

Table 1

Stored Ions : 100 keV $^{24}\text{Mg}^+$
Ring Circumference : 40 [m] ($R=6.366$ [m])
Transition energy γ_{tr} : 4.58
Tunes : $v_x=2.27, v_y=2.27, v_L=0.27$ (The same as Fig.3b)
RF Voltage V_b : 2.9 [kV]
RF frequency : 580.7 [kHz] ($h=26$)
Dispersion at the cavity η_b : 0.3 [m]
Transverse coupling strength Γ_q : 0.1

To estimate the optimum dispersion η_{opt} , we just equate Eq.(9) with $\Lambda_D/12\pi$. To obtain:

$$\eta_{opt}^2 \approx \frac{|\xi_0| R^2}{6\pi v_x \bar{v}_L^2} \left(\Lambda_D^2 + \frac{\Gamma_q^2}{v_x v_y} \right) \cot \frac{\mu_0}{2} \quad (10)$$

where we have assumed $\Lambda_D \ll 1$.

The tracking result based on the same parameters used in Fig.3(a) is given in Fig.4; effective damping is achieved. An example of parameters roughly corresponding to those of the ASTRID Ring are presented in Table 1.

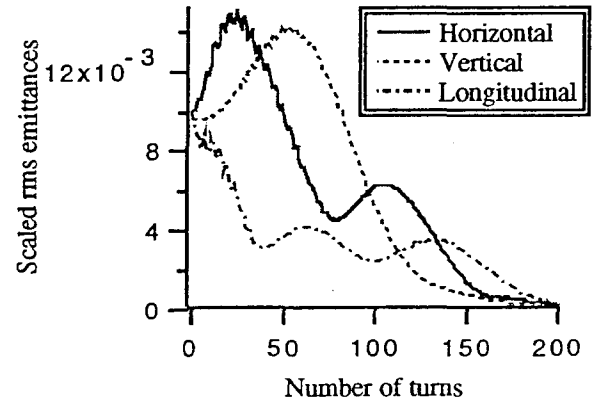


Fig.4 Tracking result corresponding to the parameters employed in Fig.3(a) with $\eta_b = 1$ m.

4. SUMMARY

We have presented two possible schemes which provide three-dimensional laser cooling. It is found that, when the operating point is on resonance, the coupling is considerably enhanced leading to large damping rates of the transverse modes. Thus, it is possible to reduce the transverse beam temperatures to a similar level to the longitudinal one.

5. REFERENCES

- [1]. D. J. Wineland and H. Dehmelt, Bull. Am. Phys. Soc. 20, 637 (1975); T. Hanchand A, Schawlow, Opt. Comm. 13, 68 (1975).
- [2]. S. Schröder et al., Phys. Rev. Lett. 64, 2901 (1990).
- [3]. J. S. Hangst et al., Phys. Rev. Lett. 67, 1238 (1991).
- [4]. H. Okamoto, A. M. Sessler, and D. Möhl, to be published in Phys. Rev. Lett.
- [5]. H. Okamoto, to be published.
- [6]. J. P. Schiffer and P. Kienle, Z. Phys. A321, 181 (1985).
- [7]. J. Wei, X-P. Li, and A. M. Sessler, submitted to Phys. Rev. Lett.
- [8]. See, for example, C. J. A. Corsten and H. L. Hagedoorn, Nucl. Instrum. Methods A212, 37 (1983).